Electronic Supplementary Material (ESI) for CrystEngComm.

Supporting Information for

Investigating water vapour sorption kinetics of aluminium MOFs by powder X-ray diffraction

Dominik Fröhlich, Philipp Hügenell and Helge Reinsch

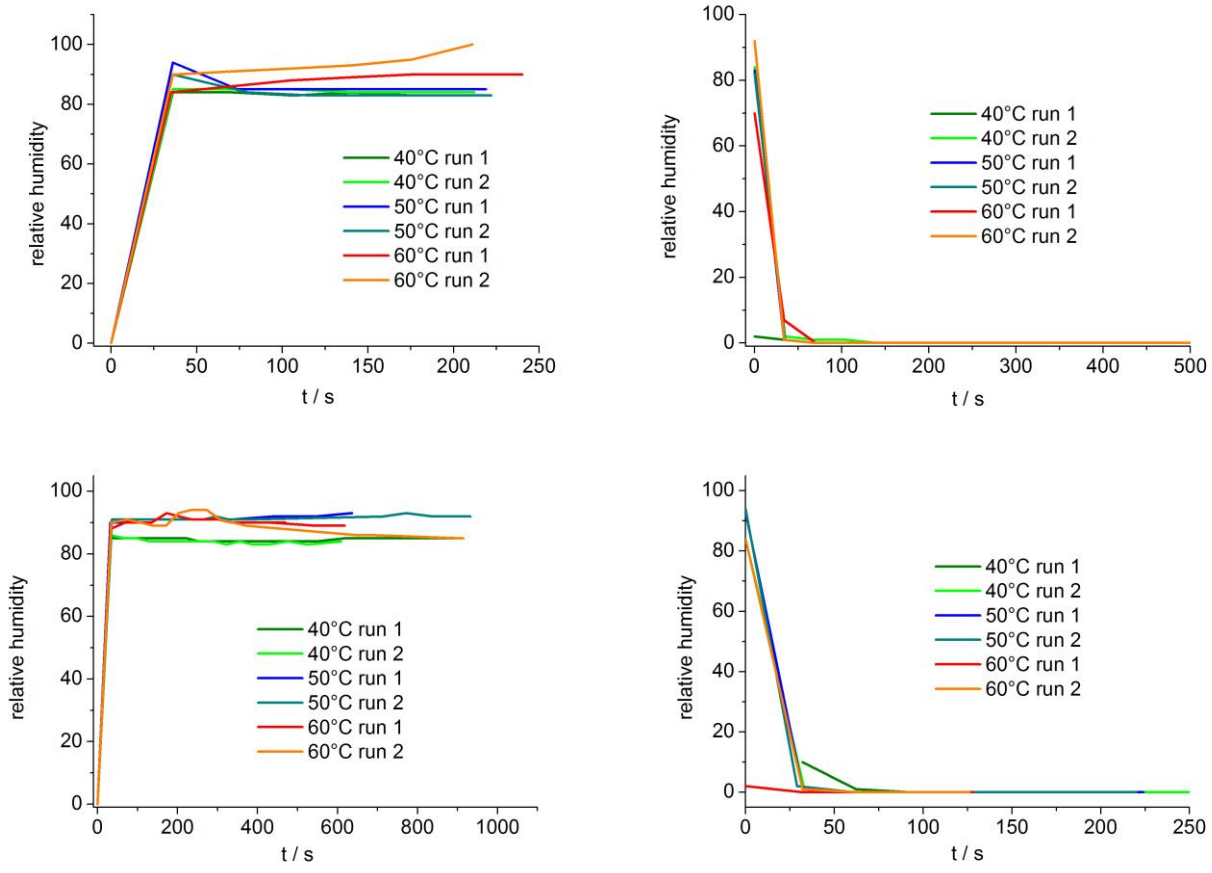

Figure S1: Relative humidities during the different runs for adsorption (left) and desorption (right) of water on CAU-10 (top)and CAU-15-Cit (bottom).

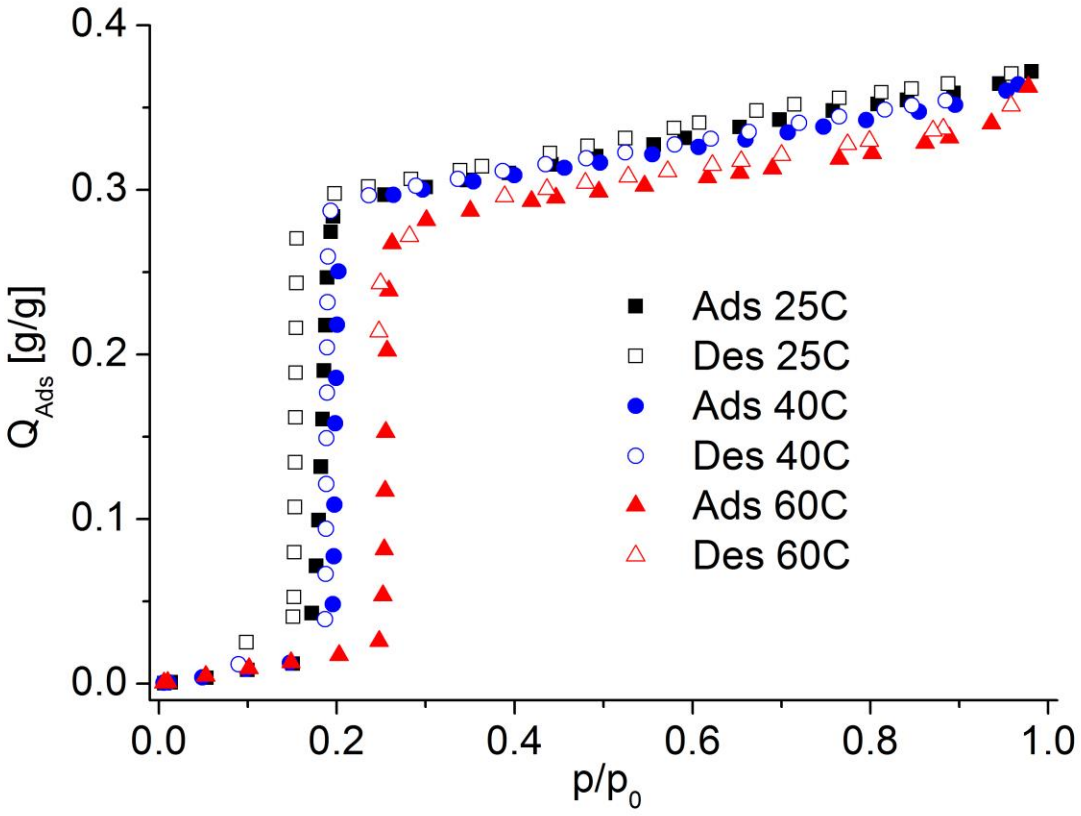

Figure S2: Volumetric water vapour sorption isotherms for CAU-10. The onset of water uptake shifts only subtly from 18 % r.h at 25°C to 22% r.h. at 40°C to 25% r.h. at 60°C.

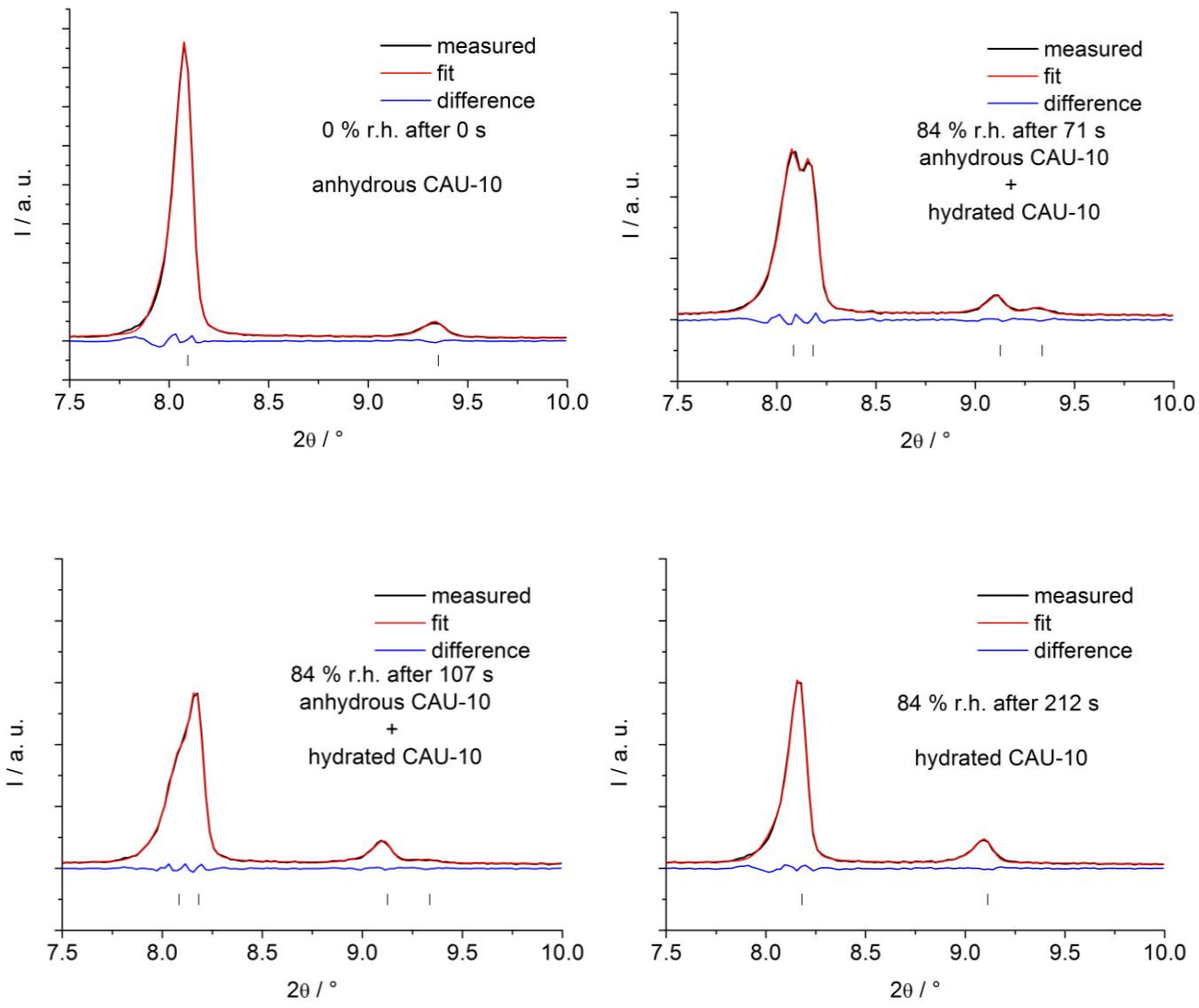

Figure S3: Peak Fits for an adsorption experiment of CAU-10 carried out at 40°C.

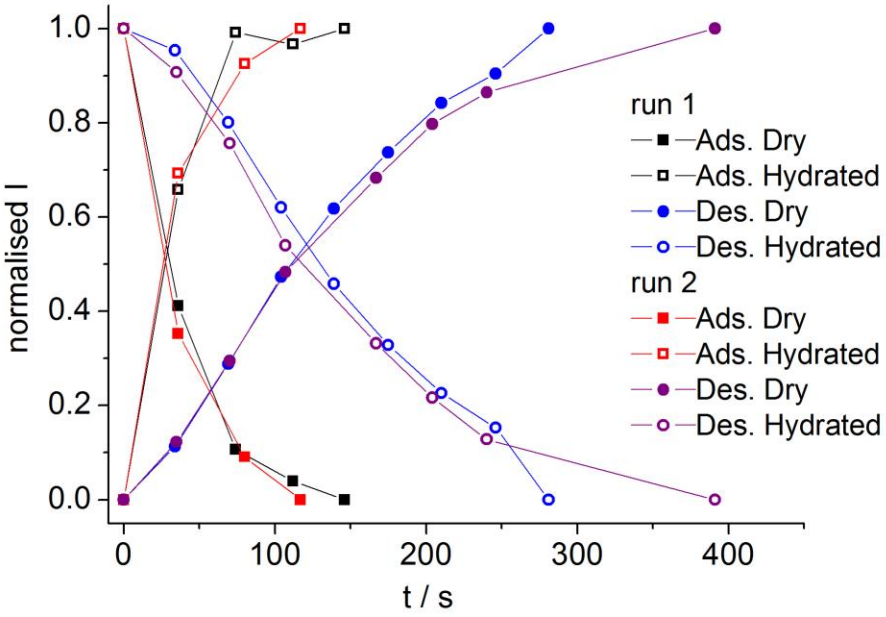

Figure S4: Plots of the normalised and integrated peak intensities for the dry CAU-10 (filled symbols) and hydrated CAU-10 (open symbols), respectively, measured during adsorption (squares, Ads.) and Desorption (circles, Des.) of two different experimental runs at 50°C.

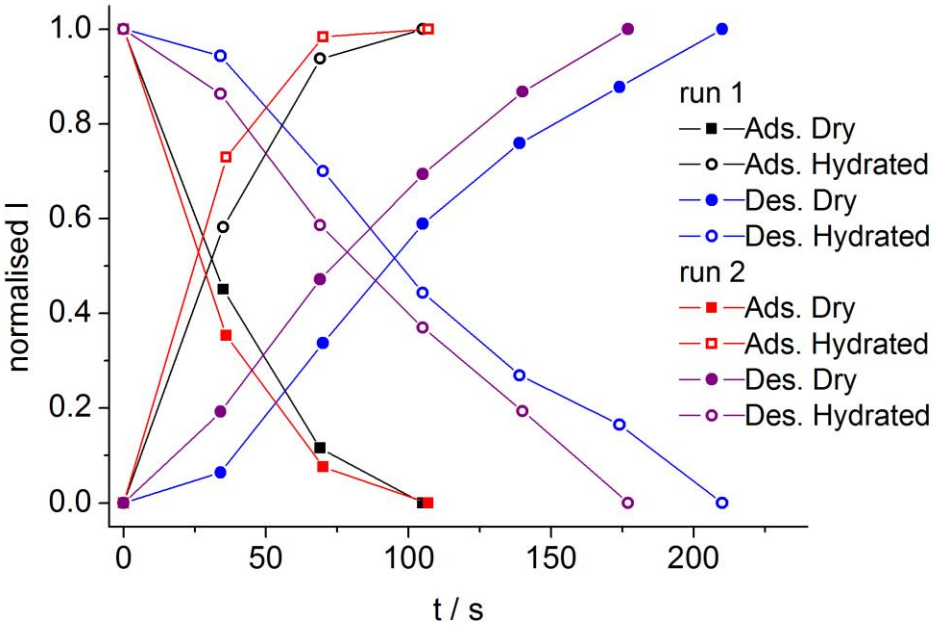

Figure S5: Plots of the normalised and integrated peak intensities for the dry CAU-10 (filled symbols) and hydrated CAU-10 (open symbols), respectively, measured during adsorption (squares, Ads.) and Desorption (circles, Des.) of two different experimental runs at 60°C. Lines are only inserted to guide the eye.

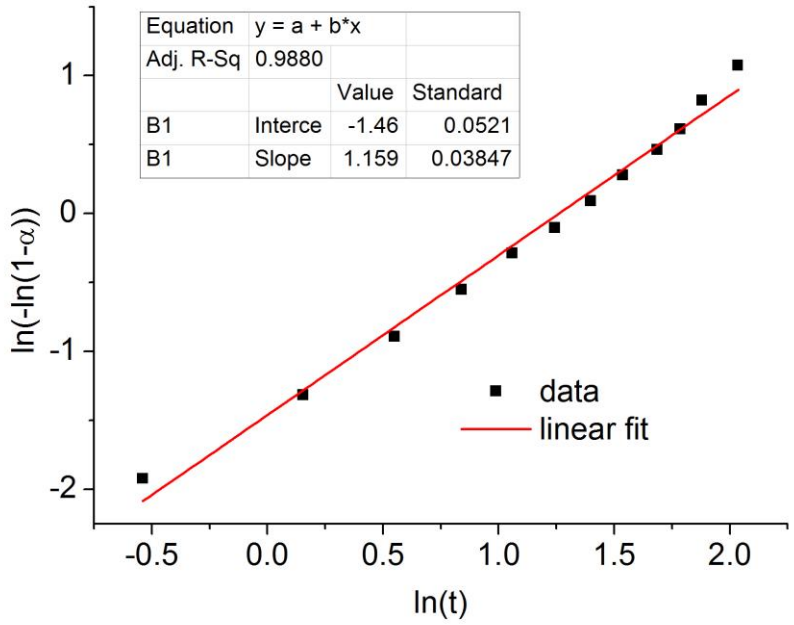

Figure S6: Sharp-Hancock plot for the first desorption run for CAU-10 at 40°C.

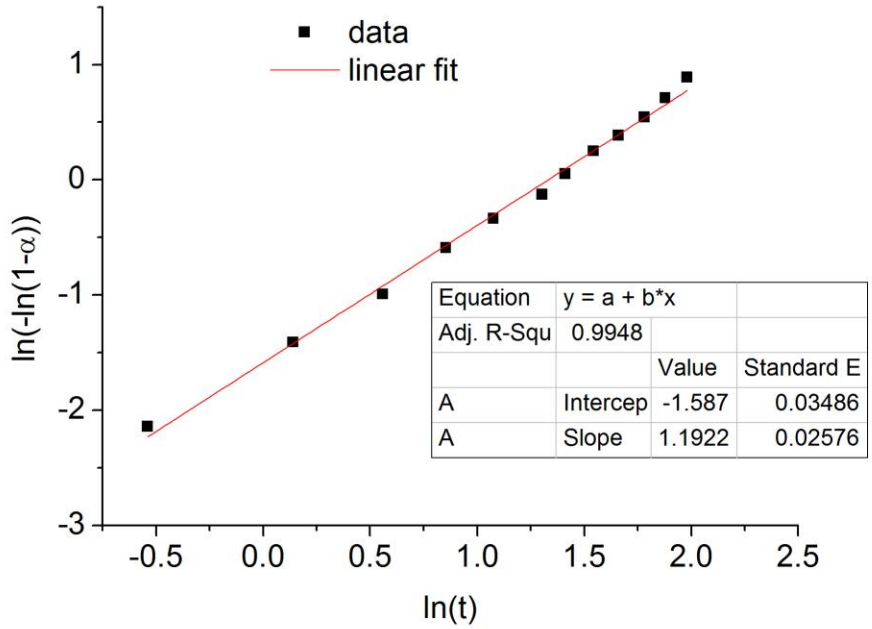

Figure S7: Sharp-Hancock plot for the second desorption run for CAU-10 at 40°C.

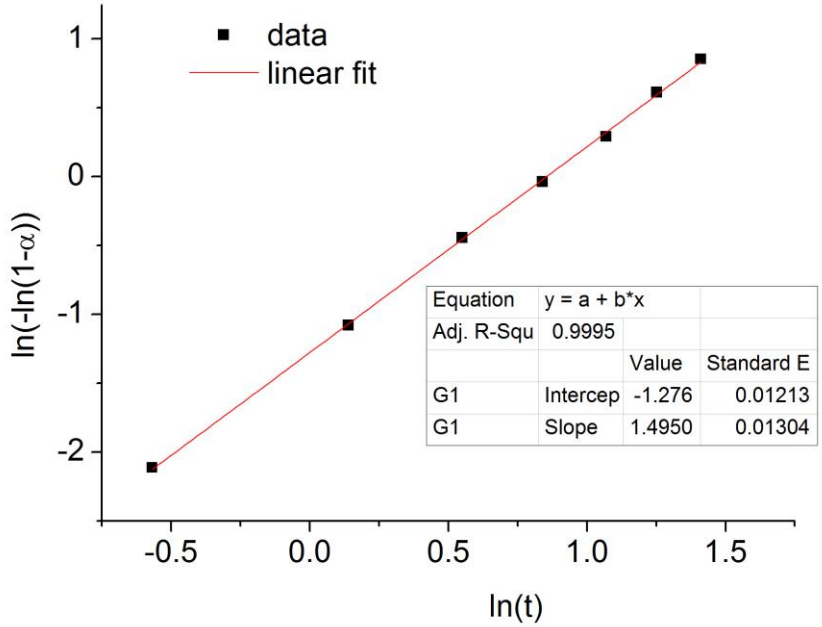

Figure S8: Sharp-Hancock plot for the first desorption run for CAU-10 at 50°C.

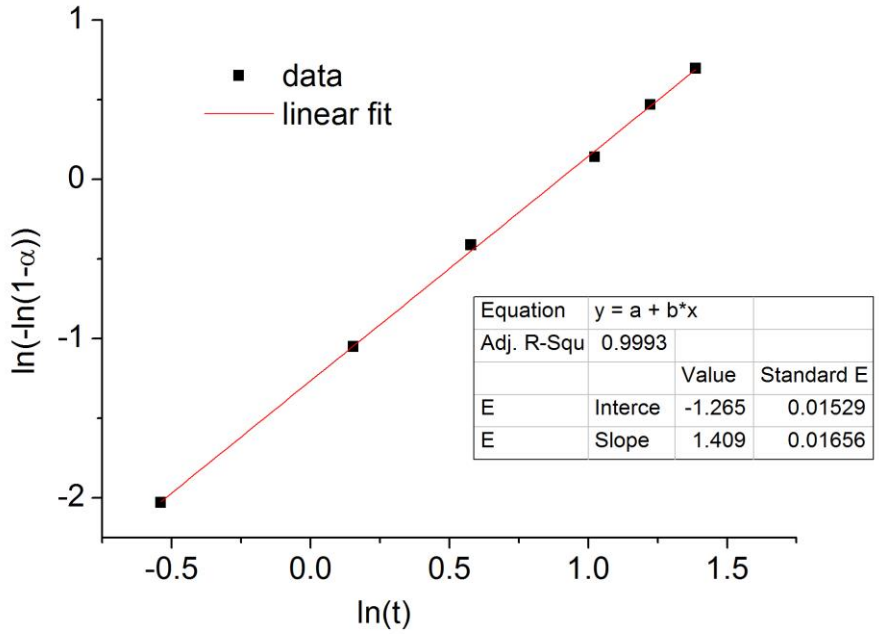

Figure S9: Sharp-Hancock plot for the second desorption run for CAU-10 at 50°C.

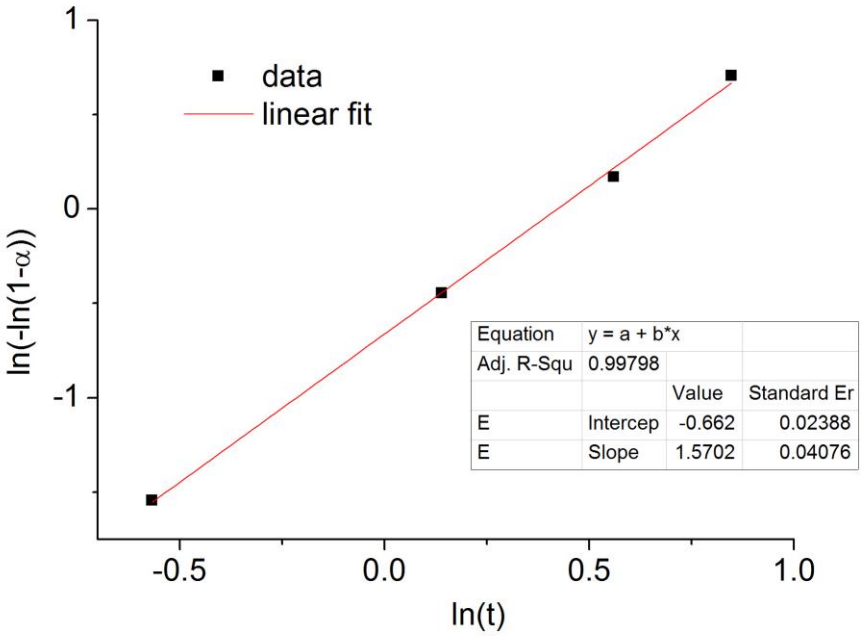

Figure S10: Sharp-Hancock plot for the second desorption run for CAU-10 at 60°C.

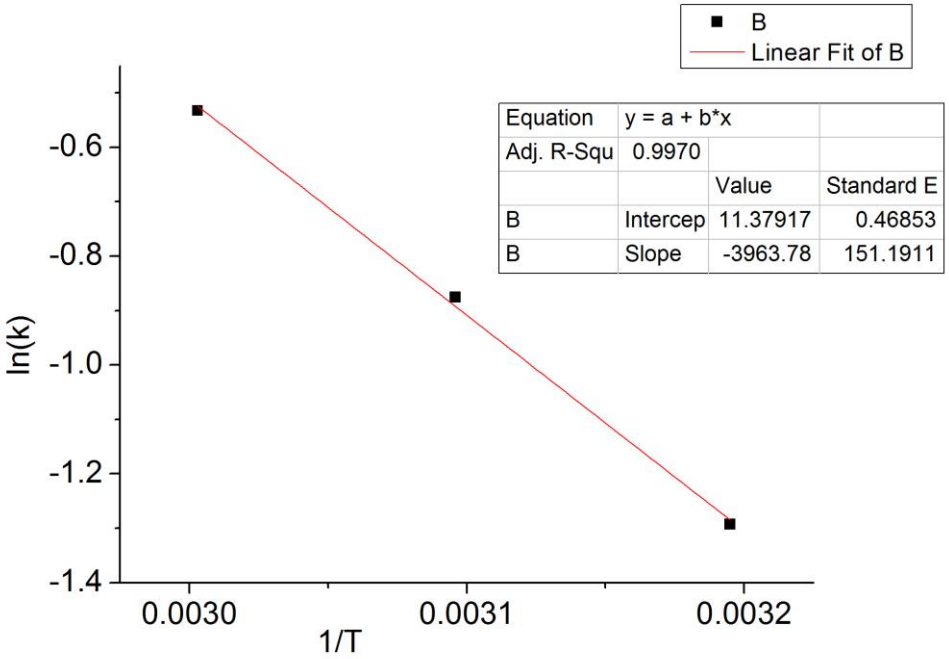

Figure S11: Arrhenius plot for the desorption of water from CAU-10.

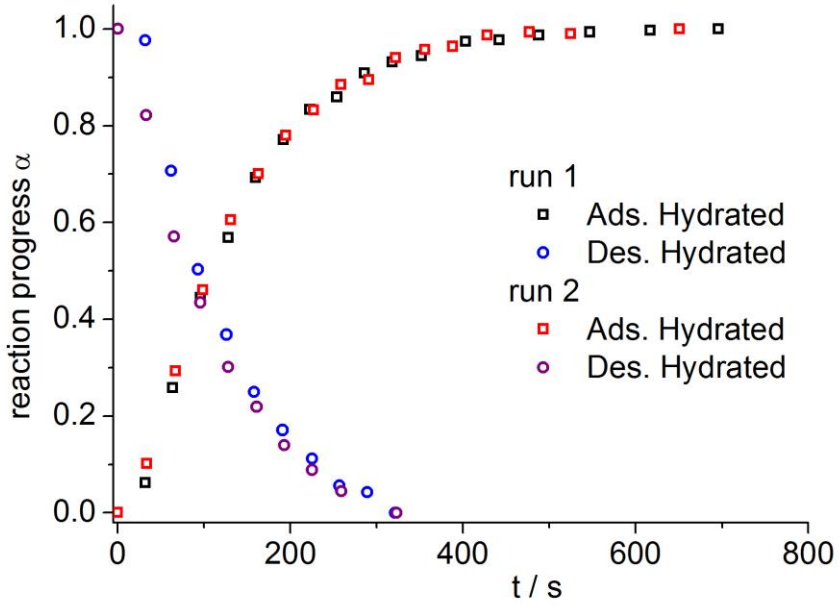

Figure S12: Plots of the normalised and integrated peak intensities for hydrated CAU-15-Cit measured during adsorption (squares, Ads.) and Desorption (circles, Des.) of two different experimental runs at 40°C.

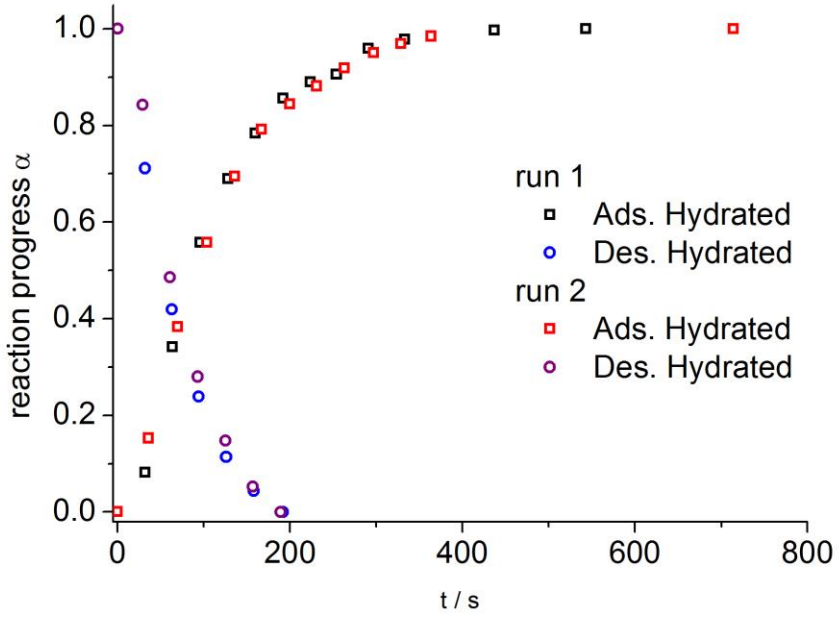

Figure S13: Plots of the normalised and integrated peak intensities for hydrated CAU-15-Cit measured during adsorption (squares, Ads.) and Desorption (circles, Des.) of two different experimental runs at 50°C.

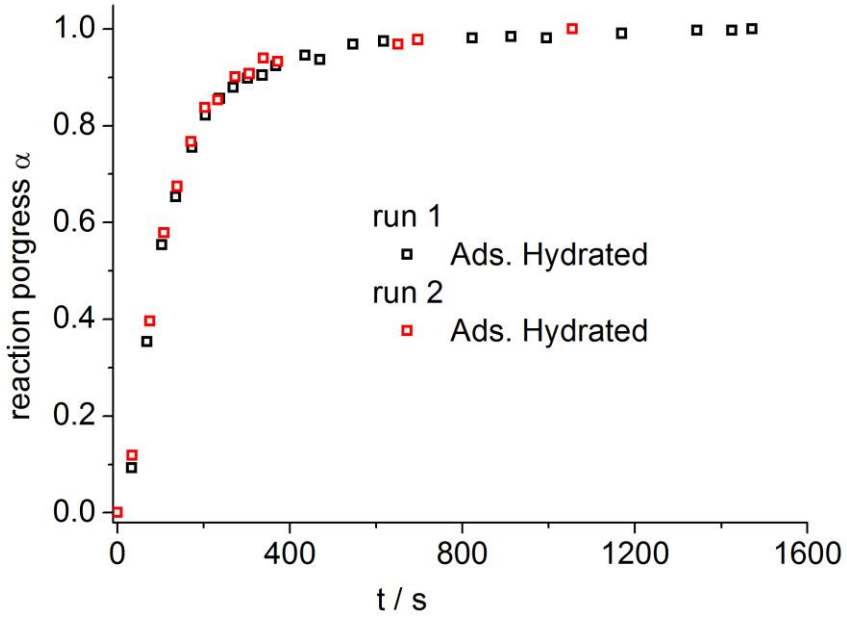

Figure S14: Plots of the normalised and integrated peak intensities for hydrated CAU-15-Cit measured during adsorption (squares, Ads.) of two different experimental runs at 60°C.

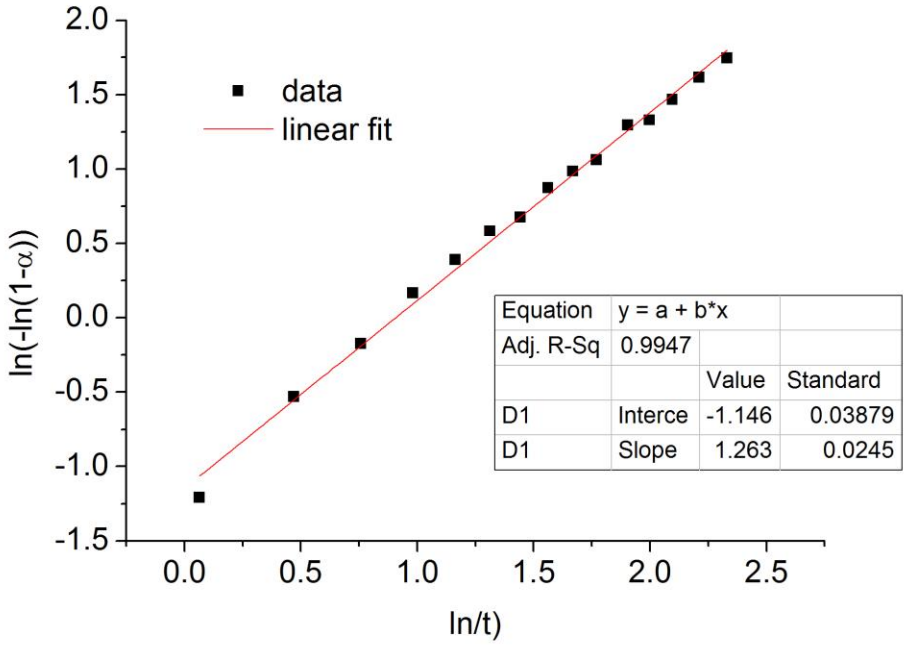

Figure S15: Sharp-Hancock plot for the first adsorption run for CAU-15-Cit at 40°C.

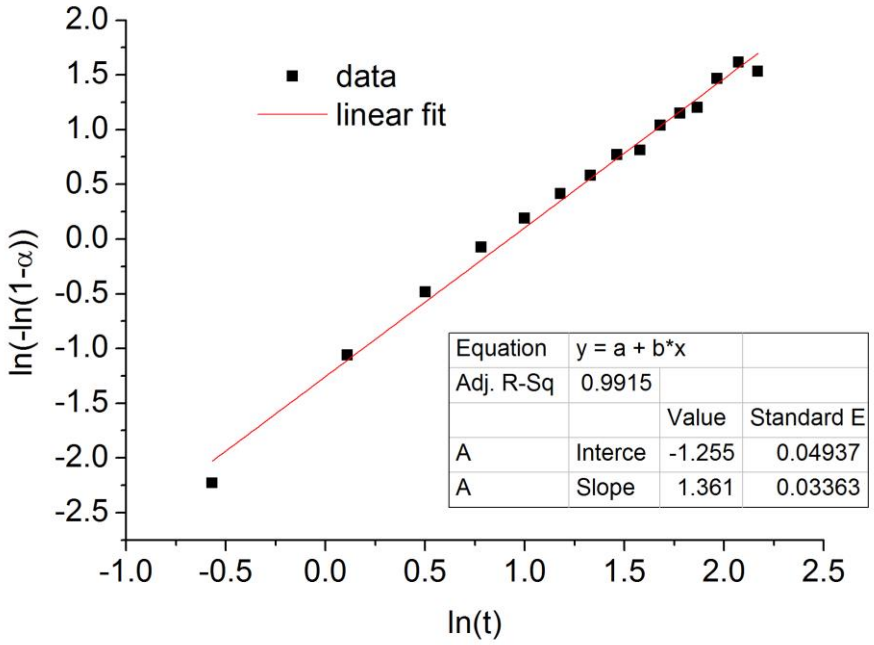

Figure S16: Sharp-Hancock plot for the second adsorption run for CAU-15-Cit at 40°C.

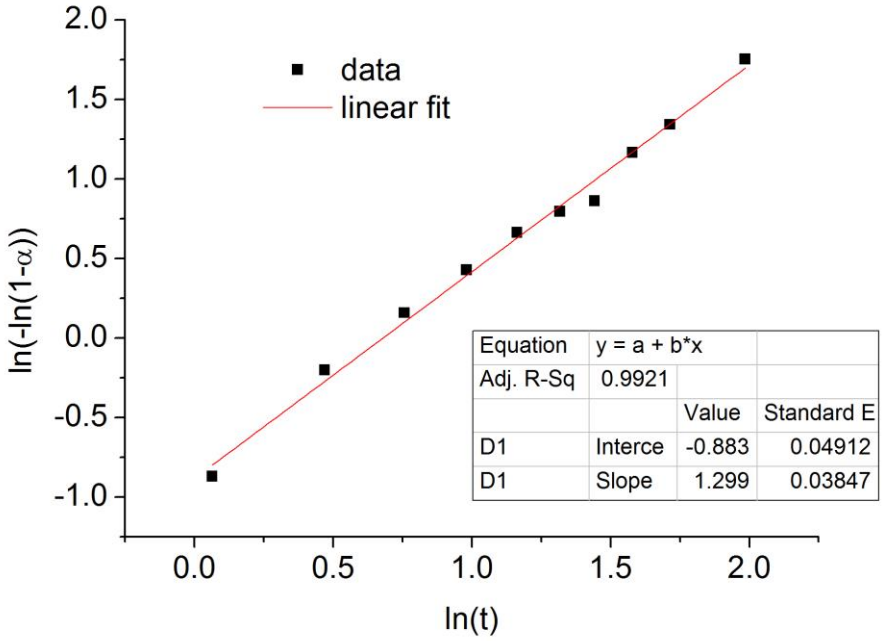

Figure S17: Sharp-Hancock plot for the first adsorption run for CAU-15-Cit at 50°C.

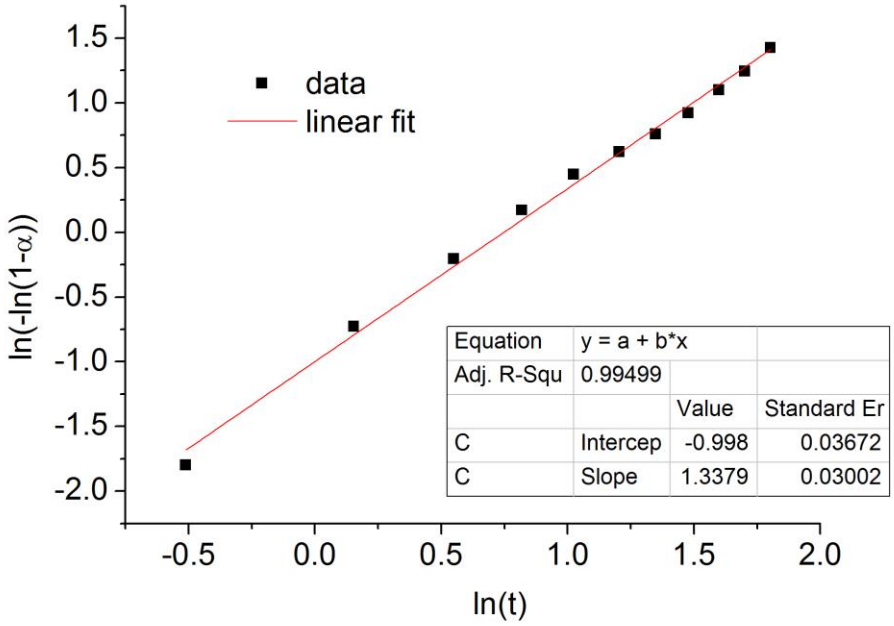

Figure S18: Sharp-Hancock plot for the second adsorption run for CAU-15-Cit at 50°C.

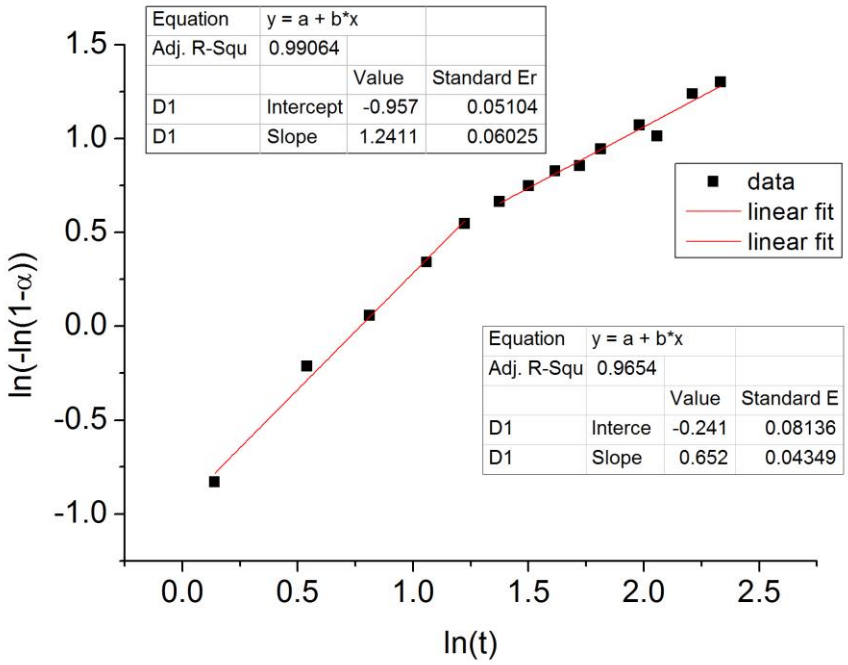

Figure S19: Sharp-Hancock plot for the first adsorption run for CAU-15-Cit at 60°C.

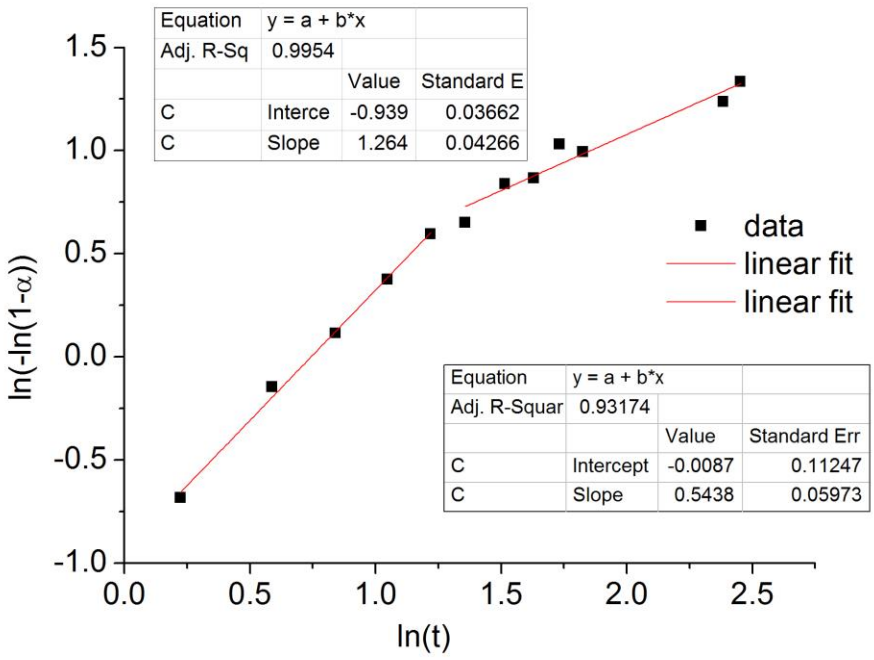

Figure S20: Sharp-Hancock plot for the second adsorption run for CAU-15-Cit at 60°C.